Hydrogen isotopes in volcanic plumes: tracers for remote temperature sensing of fumaroles

(*Geochimica et Cosmochimica Acta*, in press)

Urumu Tsunogai*, Kanae Kamimura, Saya Anzai, Fumiko Nakagawa, and Daisuke D. Komatsu

Earth and Planetary System Science, Faculty of Science, Hokkaido University
N10 W8, Kita-ku, Sapporo 060-0810, Japan

* Corresponding author. E-mail: urumu@mail.sci.hokudai.ac.jp; Tel: +81-11-706-3586; Fax: +81-11-746-0394

Keywords: volcanic plume; molecular hydrogen; isotope exchange equilibrium; remote temperature sensing

[8928 words of text with 352-word abstract and 892-word Appendix, 2 tables, 5 figures, and 74 references]

Abstract

In high-temperature volcanic fumaroles (>400°C), the isotopic composition of molecular hydrogen (H_2) reaches equilibrium with that of the fumarolic H_2O. In this study, we used this hydrogen isotope exchange equilibrium of fumarolic H_2 as a tracer for the remote temperature at volcanic fumaroles. In this remote sensing, we deduced the hydrogen isotopic composition (δD value) of fumarolic H_2 from those in the volcanic plume. To ascertain that we can estimate the δD value of fumarolic H_2 from those in a volcanic plume, we estimated the values in three fumaroles with outlet temperatures of 630°C (Tarumae), 203°C (Kuju), and 107°C (E-san). For this we measured the concentration and δD value of H_2 in each volcanic plume, along with those determined directly at each fumarole. The average and maximum mixing ratios of fumarolic H_2 within a plume's total H_2 were 97 % and 99 % (at Tarumae), 89 % and 96 % (at Kuju), and 97 % and 99 % (at E-san). We found a linear relationship between the depletion in the δD values of H_2, with the reciprocal of H_2 concentration. Furthermore, the estimated end-member δD value for each H_2-enriched component (–260±30‰ *vs*. VSMOW in Tarumae, –509±23‰ in Kuju, and –437±14‰ in E-san) coincided well with those observed at each fumarole (–247.0±0.6‰ in Tarumae, –527.7±10.1‰ in Kuju, and –432.1±2.5‰ in E-san). Moreover, the calculated isotopic temperatures at the fumaroles agreed to within 20°C with the observed outlet temperature at Tarumae and Kuju. We deduced that the δD value of the fumarolic H_2 was quenched within the volcanic plume. This enabled us to remotely estimate these in the fumarole, and thus the outlet temperature of fumaroles, at least for those having the outlet temperatures more than 400°C. By applying this methodology to the volcanic plume emitted from the Crater 1 of Mt. Naka-dake (the volcano Aso) where direct measurement on fumaroles was impractical, we estimated that the δD value of the fumarolic H_2 to be –172±16‰ and the outlet temperature to be 868±97°C. The remote temperature sensing using hydrogen isotopes developed in this study is widely applicable to many volcanic systems.

1. INTRODUCTION

The temperature of fumarolic gases provides important information about the magmatic/hydrothermal systems under the volcanoes (e.g. Giberti et al., 1992; Connor et al., 1993; Stevenson, 1993; Taran et al., 1995; Ripepe et al., 2002; Botcharnikov et al., 2003). The temperature often increases prior to eruptions or during shallow intrusions of magma (e.g. Menyailov et al., 1986). Thus, measurements of fumarole outlet temperature have been carried out extensively to understand magmatic processes and to detect the precursors of eruptions.

However, direct measurements on fumaroles are often neither practical nor safe. Remote sensing using infra-red (IR) wavelengths of surface temperatures offers an alternative to direct measurement. This technique has been applied to a variety of volcanoes since the early 1960s (e.g. Fischer et al., 1964; Shimozuru and Kagiyama, 1976; Saito et al., 2005; Harris et al., 2009).

Thermometers using IR remote sensing, however, have several problems when applied to the determination of outlet temperatures of active volcanic fumaroles: (1) IR remote sensing determines the average temperature for each pixel. When a fumarole has surface dimensions smaller than the pixel, the measured temperature becomes the average temperature of an area including low temperature ground surrounding the fumarole. As a result, the measured temperature is inaccurate for that of the fumarole; (2) Line-of-sight is necessary for these thermometers, this is difficult when the fumarole is obscured, *e.g.* by fogs, rocks, and ejecta (volcanic clouds and ash), (3) absorption of the IR radiation by gases emitted from fumaroles (*e.g.* H_2O and CO_2) gives low accuracy and precision of measured temperatures; (4) non-measurement IR radiation (solar, or ground radiation) can also give low accuracy and precision of the measured temperature. Thus, we developed an alternative method to determine the temperature of distant volcanic fumaroles using geochemical tracers in the volcanic plume.

Because of rapid reactions between fumarolic components at high temperatures, fumarolic gases often attain chemical and isotopic equilibrium close to the outlet (*e.g.* Ellis, 1957; Matsuo, 1961; Giggenbach, 1987; Shinohara *et al*., 1993; Ohba *et al*., 1994; Symonds *et al*., 1994). In particular, for the hydrogen isotope exchange reaction between H_2O and H_2 in fumaroles at outlet temperatures greater than 400°C, the calculated isotope temperatures (assuming hydrogen isotope exchange equilibrium between H_2O and H_2; see section 3.3 for the details of the calculation) were close to the actual outlet temperatures (e.g. Bottinga, 1969; Mizutani, 1983; Kiyosu and Okamoto, 1998; Taran et al., 2010).

$$H_2O + HD \leftrightarrow HDO + H_2 \qquad (1.1)$$

For example, the fumarole outlet temperatures of both the Showashinzan and Nasudake volcanoes have declined, from 800°C in 1954 to 617°C in 1977, and from 489°C in 1960 to 277°C in 1969, respectively. Consistent with these declines, the calculated isotope temperatures also declined, from 750°C to 630°C at Showashinzan and from 470°C to 290°C at Nasudake (Mizutani, 1983). A similar agreement between the calculated isotope temperatures and the outlet was found in subaerial/submarine hydrothermal fluids showing the temperatures more than 200–300 °C (e.g. Kiyosu, 1983; Welhan and Craig, 1983; Proskurowski et al., 2006; Kawagucci et al., 2010). These past observations of fumarolic H_2 suggest that the isotope exchange reaction is rapid enough at the outlet temperature to re-equilibrate the calculated isotope temperature to the outlet temperature of the volcanic fumarole, irrespective of the origin of H_2O and H_2 in the fumarole. Furthermore, the isotope exchange reactions slow down sufficiently after cooling that the D/H ratio is effectively "frozen" at the D/H ratio just before sampling.

Similar processes that result in the re-equilibration of the hydrogen isotopes and subsequent "freezing" of that re-equilibration can also be anticipated in volcanic plumes. If we could estimate the hydrogen isotopic compositions of both the H_2O and H_2 in the fumaroles from those in the volcanic plume, it would be possible, by assuming the isotope

79 exchange equilibrium in fumarolic H_2O and H_2, to remotely deduce the temperature of the
80 fumaroles. Within the possible isotope fractionations among the major components in
81 fumarolic gases, the hydrogen isotope fractionation between H_2O and H_2 has the largest
82 fractionation factor under the isotope exchange equilibrium, as well as the largest
83 temperature-dependent variation (Richet *et al.*, 1977), so that the temperature estimation using
84 hydrogen isotopes can be precise.

85 While H_2 is one of the major components in high-temperature fumarolic gases (0.1 to
86 3% by volume (including H_2O), Symonds *et al*., 1994), H_2 is depleted in atmosphere, present
87 at concentrations of *ca*. 0.5 ppm in tropospheric air (Novelli *et al*., 1999). Hence, the volcanic
88 plume has an excess of H_2 relative to the troposphere (McGee, 1992; Symonds *et al.*, 1994).
89 Consequently, we can estimate the D/H ratio of fumarolic H_2 from the concentrations and
90 D/H ratios of the H_2 in the volcanic plume, by subtracting atmospheric contributions to the
91 D/H ratios of the H_2 in the volcanic plume (see section 4.2 for the detail). It is more difficult
92 to estimate D/H ratios of fumarolic H_2O from those in plume because of possible enrichment
93 of H_2O in tropospheric air. However, it turns out that we can assume the D/H ratios without
94 actual measurements (see sections 4.3 and 4.4 for the detail). As a result, we can estimate the
95 outlet temperature of fumaroles, from the D/H ratios of the fumarolic H_2 (determined) and the
96 fumarolic H_2O (assumed).

97 In this study we determined both the concentrations and D/H ratios of H_2 in volcanic
98 plumes emitted from fumarolic areas in active volcanoes in Japan, together with those from
99 high-temperature fumaroles wherefrom the plumes are derived, to verify that:

100 (1) H_2 from high-temperature fumaroles attain isotope exchange equilibrium with
101 co-existing fumarolic H_2O, and,

102 (2) the D/H ratios of fumarolic H_2 are “frozen” in the plume, and, that we can deduce
103 them from those in volcanic plume.

Furthermore, we applied this new methodology to a volcanic plume emitted from a fumarolic area where direct temperature measurements were difficult, to estimate the D/H ratio of fumarolic H_2 and thus the outlet temperature of fumaroles remotely. As far as we are aware, this is the first report of a D/H ratio from H_2 in a volcanic plume. This work has been made possible by recent advances in stable isotope measurements using Continuous-Flow Isotope Ratio Mass-Spectrometry (CF-IRMS), which enabled us to make such highly sensitive measurements on the D/H ratios of H_2 close to the atmospheric levels without any cumbersome and time-consuming pretreatments (Rahn et al., 2002; Rhee et al., 2004; Rice et al., 2010).

2. GEOLOGICAL BACKGROUND

In this study, samples of high-temperature fumarolic gases were taken from 3 surface volcanic fumaroles, together with the samples of volcanic plumes derived apparently from the fumaroles, in the active volcanoes of Tarumae, Kuju, and E-san. Additionally, plume samples emitted from the Crater 1 of the volcano Mt. Naka-dake in Aso were taken, where neither direct sampling of fumarolic gases nor direct measurement of the outlet temperature at the fumaroles on the floor of the crater were possible. The locations of the studied volcanoes are presented in Figure 1.

Tarumae volcano

The Shikotsu caldera (13 × 15 km), largely filled by the waters of Lake Shikotsu, was formed during one of the largest Quaternary eruptions about 31 to 34 KY BP in Hokkaido Island, Japan (Fig. 1). The small andesitic Tarumae stratovolcano was then constructed on the south-eastern rim and has been Hokkaido's most active volcano since. The Tarumae volcano is now capped by an andesitic flat-topped summit lava dome that formed in 1909, having the diameter of 450 m and the height of 130 m. There are 7 major fumarolic vents in and around the summit lava dome, named A, B, C, D, E, F, and G. Vent A is located on the south-eastern

130 flank of the lava dome and is presently one of the most active fumarolic areas on the Tarumae
131 volcano. Previously, this had been a huge vent having a inner diameter of more than a meter,
132 so that no data had been reported for the chemical composition of exiting gases, except for
133 estimations from the volcanic plume (Shinohara, 2005). However, the inner wall of Vent A
134 collapsed in 2004 so that most of the main vent has been buried by the debris. Now, an
135 intense gas emission occurs from many tiny fumaroles at the bottom of a crater about 5 m
136 deep with a 10 m diameter. In this study, the samples for analysis were taken in and around a
137 fumarole in Vent A.

138 *Kuju volcano*

139 Kuju volcano consists of 20 lava domes and cones, located in the central part of Kyushu
140 Island, Japan (Fig. 1). One of the most active fumarolic areas in the volcano is Mt. Iwoyama,
141 situated on the north-eastern flank of Mt. Hossho, where sulfur used to be mined. The
142 fumarolic area consists of 4 fields named A, B, C, and D. The fields A, B and C were
143 pre-existent, and in older literature named “KX”, “KO”, and “KH”, respectively. (*e.g.*
144 Mizutani *et al*., 1986). Field D on the other hand is a group of new vents (named a, b, c, d and
145 e) that were opened by the phreatic eruption of 1995.

146 Temporal variations were observed in the chemical and isotopic compositions of the
147 fumarolic gases in Field C (the KH field) between 1959 and 1984 and were attributed to the
148 increase in the mixing ratios of meteoric water with magmatic gases (Mizutani *et al*., 1986).
149 On the other hand, temporal variations were small for Fields A and B (Mizutani *et al*., 1986;
150 Amita and Ohsawa, 2003). All the samples for analysis from the Kuju volcano were taken in
151 and around a fumarole in Field A.

152 *E-san volcano*

153 The E-san volcano, a small andesitic stratovolcano capped by a 618-m-high lava dome,
154 is located in southernmost part of Hokkaido Island, Japan (see Fig. 1). The E-san volcano
155 occupies the eastern tip of the double-pronged Oshima Peninsula across the Tsugaru Strait

from Honshu. The lava dome of the E-san volcano, which formed about 9 KY BP, and the volcano has been active during the Holocene. A minor phreatic eruption in 1846 produced a mudflow that caused many fatalities. The most recent activity at E-san was a small eruption in 1874. Active fumaroles at temperatures of up to 225°C occur in fumarolic areas on the upper northwestern flank (Y field) and the middle western flank (X field). These are located about 400 m apart. Past studies on the fumarolic gases revealed that discharges were dominated by magmatic water and gases (Matsubaya *et al*., 1978; Hedenquist and Aoki, 1991).

All the samples for analyzing fumarolic gases from the E-san volcano were taken at one of the active fumaroles in the X field. The plume samples were taken around the fumarole.

Aso volcano

The Aso volcano is a volcanic caldera located in the central part of Kyushu Island, Japan (see Fig. 1). It was formed during the major explosive eruptions between 300 KY BP and 90 KY BP. A group of 17 central cones formed in the middle of the caldera, one of which, Mt. Naka-dake, is one of the most active volcanoes in Japan. It was the location of Japan's first documented historical eruption in 553 AD.

The active crater located in the Mt. Naka-dake, named as the Crater 1 of Mt. Naka-dake, is about 400 m in diameter, (see Fig. 2). The active fumarolic area is located at the bottom of the Crater 1, about 80 m below the crater edge, (see Fig. 2). Neither direct sampling of fumarolic gases nor direct measurements of fumarolic temperature were practical in this deep crater. In this study, the samples of volcanic plume were taken at the points A to F (see Figure 2).

3. METHODS

3.1 Sampling

The samples were taken at Tarumae on 6 October, 2010, Kuju on 11 November, 2010, E-san on 19 June, 2010, and Aso on 10 November, 2010. Prior to sampling the fumarolic gases, we measured the temperature of fumaroles as many fumaroles as possible to choose the fumarole that exhibited the highest outlet temperature within each fumarolic area. The highest temperature of the fumaroles in each fumarolic area, where the fumarolic gas samples were taken, were 609°C at Tarumae, 203°C at Kuju, 107°C at E-san (Table 1).

A quartz pipe and silicone rubber tubing were used to introduce the fumarolic gases into sampling bottles, after flushing them with sample for more than 15 minutes. Then, the fumarolic gases were introduced into a 100 mL glass syringe with two mouths via condensation traps made of Pyrex glass (ca. 300 mL) cooled to 0°C. The gases were sucked into the trap by syringe. The water content of the sample was determined from the difference in weight of the trap before and after sample collection. The volume of dried fumarolic gases relative to the water content was determined from both inner volume of the syringe (100 mL) and the number of strokes. The water sample in the condensation traps was stored in polypropylene bottles for later analysis on D/H ratios. The dried fumarolic gases in the glass syringe were introduced via the needle into a pre-evacuated glass vial with a butyl rubber septum stopper (20 to 65 mL). These samples were analyzed for both H_2 concentrations and D/H ratios. This method was found to preserve fumarolic H_2 samples for more than a month, without detectable changes in either the concentrations or D/H ratios.

Additional to the description above, samples of fumarolic gases were introduced into pre-evacuated 140 mL glass bottles containing 10 mL of 5 mol/L NaOH solution (ultra pure grade) (Giggenbach and Goguel, 1989). These samples were used to determine concentrations of H_2O and H_2 in fumarolic gases. Acidic components of the fumarolic gases dissolved in the NaOH solution, whereas the other non-acidic gases such as H_2 remained in the head space. H_2 concentrations in the fumarolic gases were determined from those in head space. H_2O concentrations in the fumarolic gases were determined from the increase in the volume of the

NaOH solution. D/H ratios of H_2 in the head space were measured as well. However, these changed toward D enrichment with storage beyond the analytical precision (a few ‰ per day). Hence, we did not include the D/H ratios of H_2 obtained through this method in the final results.

The samples of each volcanic plume were taken into pre-evacuated 300 mL glass bottles with two stopcocks (sealed by o-rings made of Viton) at both ends. These were filled to atmospheric pressure (Tsunogai *et al*., 2003). Samples were taken by moving away from each targeted fumarole, along the line of the plume. Approximate distances to each targeted fumarole for each sampling point are shown in Table 2. We also took samples of background air at each site, at a point distant from the fumarolic area and if possible upwind (Table 2). The wind speed during sampling was always less than 2 m/s.

3.2 Analysis

Concentrations and D/H ratios of H_2 were determined using the CF-IRMS system at Hokkaido University (*e.g.* Tsunogai *et al*., 2002; Ishimura *et al*., 2004; Kawagucci *et al*., 2005; Komatsu *et al*., 2005; Komatsu *et al*., 2008; Hirota *et al*., 2010). This system consists of an original helium-purged pre-concentration system for H_2 and a Delta V Advantage (Thermo Fisher Scientific, Waltham, MA, USA) with a modified GC-C/TC III interface and Thermo Trace GC ULTRA gas chromatograph. The analytical procedures are outlined below, details will be presented elsewhere.

For each measurement, a gas sample of appropriate volume (250 mL at STP for a 0.5 ppm plume sample, and 0.25 mL at STP for a 5,000 ppm fumarolic gas sample, where ppm means parts per million by volume), was introduced into our original stainless steel line (pre-flushed with carrier gas stream of ultra pure helium). In this line, H_2 in each sample was purified from the other coexisting components, such as O_2, Ar, N_2, CH_4, CO_2, SO_2, H_2S, and H_2O, by passing the sample through a cold condensation trap (4 mm ID) held at –197°C and a

column (4 mm ID) packed with Molecular sieve 5A held at –110°C. The H_2 was gathered onto the head of a column (2 mm ID) packed with Molecular sieve 5A held at –197°C and where the carrier pressure was greater than 3,000 Torr. The temperature of the column was then ramped up to room temperature, and the eluted H_2 portion was concentrated again at the head of an HP-PLOT Molsieve capillary column (30 m, 0.32 mm ID) held at –197°C (Tsunogai *et al.*, 2002). The column head was then quickly heated to room temperature under a continuous helium flow rate of 0.4 mL/min and the column-separated H_2 was passed into a mass spectrometer to determine both content and D/H ratios by simultaneous monitoring of the masses of H_2^+ (m/z=2) and HD^+ (m/z=3). We introduced pure H_2 before and after the sample H_2 peak, as a calibration standard for the D/H ratios (Tsunogai *et al*., 2002).

Following provisional IUPAC recommendations (Coplen, 2008), the δ-notation is used in this paper to denote D/H ratios (δD) as defined by the following equation:

$$\delta D = \frac{R_X}{R_{STD}} - 1 \qquad (3.1)$$

where R_X denotes the D/H ratio of a sample and R_{STD} denotes the D/H ratio of standard material. Unless otherwise noted, we used VSMOW (Coplen and Hopple, 1995) as for the standard material to present δD values in this paper. Within the text, usual δD values are presented using the traditional ‰ (*i.e.* 10^{-3}). Please therefore note that a δD value of +5‰, for instance, means +0.005.

Whilst quantifying samples, as a quality control measure we also analyzed a working-standard gas mixture containing H_2 of known concentration (221 ppm) and known $\delta D(H_2)$ values at least once a day in the same manner as the samples themselves. The δD values of H_2 in the working-standard gas mixture were precisely calibrated by using commercial standards of pure H_2. By using the peak area ratios of m/z 2 vs. 3, we calculated the δ value between the sample and the running standard during sample analysis. For normalization to the international standard, the following relation was applied:

$$\delta_{sa-std} = \delta_{sa-rs} + \delta_{rs-std} + \left(\delta_{sa-rs} \times \delta_{rs-std}\right) \qquad (3.2)$$

where $\delta_{rs\text{-}std}$ is the δD value for the running standard against the international standard, which was determined from the measurement of the working-standard gas mixture that contains H_2 of known δD compositions ($\delta_{ws\text{-}std}$) via the following calculation:

$$\delta_{rs-std} = \frac{\delta_{ws-std} - \delta_{ws-rs}}{\delta_{ws-rs} + 1} \qquad (3.3)$$

The concentration of H_2 in a sample was calculated by comparing each H_2 peak area with that of the working standard gas mixture. The error of the determined concentrations was estimated to be <3%. An analytical precision of 4‰ for δD was achieved for samples containing as little as 5 nmol H_2 within the one hour required for a single sample analysis. Total analytical blank associated with the method was estimated to be ca. 50 pmol for H_2 having the δD value of +1300‰ using the method described in Gelwicks and Hayes (1990). These were subtracted from the final concentrations and δD values of H_2.

The stable hydrogen isotopic compositions of H_2O ($\delta D(H_2O)$) were determined using the same CF-IRMS system in Hokkaido University, after converting 0.5 μl of sample H_2O to H_2 using chromium at 880°C under vacuum condition (Itai and Kusakabe, 2004). A portion (about 2%) of H_2 was sub-sampled and introduced into the stainless steel line while flushing with the carrier gas stream of ultra pure helium. It was pre-concentrated on the head of a column (2 mm ID) packed with Molecular sieve 5A held at –197°C. Subsequent procedures were the same with the $\delta D(H_2)$ analysis. In addition to analyzing the samples, we also analyzed our internal working-standards (filtered deep-sea water, filtered tap water, and filtered Antarctic ice water, each having known $\delta D(H_2O)$ values). We did these measurements at least twice every day in the same manner as the samples themselves to calibrate the $\delta D(H_2O)$ values of sample to the international scale. The δD values of the working-standards had been precisely calibrated by using international standards of VSMOW and VSLAP

(Coplen and Hopple, 1995). An analytical precision of 0.8‰ for δD can be achieved for a single sample analysis within the 20 minutes required for analysis.

3.3 Calculation of apparent equilibrium temperature

By using the temperature-dependent variation in the equilibrium fractionation factor of hydrogen isotopes between H_2O and H_2 ($\alpha_{H2O\text{-}H2}$), we can estimate the apparent equilibrium temperature (isotope temperature) for δD (AET_D) from the values of $\delta D(H_2O)$ and $\delta D(H_2)$, assuming hydrogen isotope exchange equilibrium between H_2O and H_2 (*i.e.* $\alpha_{H2O\text{-}H2} = (\delta D_{H2O}+1)/(\delta D_{H2}+1)$). In this study, AET_D less than 1,000 °C is estimated from $\alpha_{H2O\text{-}H2}$ using the following equation (3.4), which we obtained through least squares fitting to the relationship between AET_D (°C) and $10^3\times\ln(\alpha_{H2O\text{-}H2})$ as presented in Richet et al. (1977):

$$AET_D = \left\{4.474\times10^{-12}\times\Delta^2 + 3.482\times10^{-9}\times\Delta + 9.007\times10^{-8}\right\}^{-\frac{1}{2}} - 273.15 \qquad (3.4)$$

where Δ represents $10^3\times\ln(\alpha_{H2O\text{-}H2})$. The relationship between AET_D and $10^3\times\ln(\alpha_{H2O\text{-}H2})$ is schematically shown in Fig. 3.

4. RESULTS & DISCUSSION

4.1 H_2 in Fumaroles

The chemical and isotopic compositions of the fumarolic gases are presented in Table 1. The concentrations of H_2 were expressed relative to H_2O concentration in μmol/mol. Both H_2/H_2O ratios and $\delta D(H_2O)$ values agreed well with those reported for each volcano in past studies. For example, Mambo and Yoshida (1993) reported H_2/H_2O ratios of 430±340 μmol/mol for a 232°C fumarole at Vent B (Tarumae) (recalculated from their data assuming the mixing ratio of H_2 within the total non-acidic gases, such as H_2, N_2, He, CH_4, CO and Ar, to be 50±40%, in which most of high-temperature fumarolic gas data are included; Symonds et al., 1994). For Kuju, Amita and Ohsawa (2003) reported H_2/H_2O ratio of 41.8 μmol/mol

and $\delta D(H_2O)$ value of –49.9‰ for a 157°C fumarole in Field A, Saito *et al*. (2002) reported H_2/H_2O ratios of ca. 70 μmol/mol and $\delta D(H_2O)$ values of ca. –50‰ for a 351°C fumarole in Field C, and Mizutani *et al.* (1986) reported H_2/H_2O ratio of 5 (μmol/mol) and $\delta D(H_2O)$ value of –37‰ for a 165°C fumarole in Field A. At E-san, Mambo and Yoshida (1993) reported H_2/H_2O ratios of 360±290 μmol/mol for a 225°C fumarole (recalculated from their data assuming H_2 occupies 50±40% of the non-acidic gases) and Matsubaya *et al*. (1978) reported $\delta D(H_2O)$ values of –32‰ and –36‰ for fumaroles showing temperatures of 157 and 185°C, respectively, and Hedenquist and Aoki (1991) reported $\delta D(H_2O)$ values from –50 to –30‰ for fumaroles at 100 to 225°C. Taking into account that both H_2/H_2O ratios and $\delta D(H_2O)$ values tend to increase with both outlet temperatures (e.g. Matsuo, 1961; Symonds et al., 1994; Goff and McMurtry, 2000; Botcharnikov et al., 2003) and mixing ratios of magmatic water relative to meteoric water (e.g. Mizutani et al., 1986; Goff and McMurtry, 2000; Botcharnikov et al., 2003), our data on the H_2/H_2O ratios and the $\delta D(H_2O)$ values (see Table 2) are not unreasonable for those of fumarolic discharges from these volcanoes. The $\delta D(H_2O)$ values imply that local meteoric water also contributed to fumarolic H_2O, especially at Kuju. The mixing ratios, however, were always less than 50 %. That is to say, the major portion of fumarolic H_2O was magmatic in these fumaroles.

The $\delta D(H_2)$ values in Table 2 were reasonable for those of high-temperature fumarolic discharges. Past studies show that the H_2 in fumarolic discharges re-equilibrated with coexisting fumarolic H_2O at outlet temperature greater than 400°C (*e.g.* Bottinga, 1969; Mizutani, 1983). The observed outlet temperatures are presented in Table 1, together with the AET_D calculated from the values of $\delta D(H_2O)$ and $\delta D(H_2)$ in each fumarolic gas sample. Besides, the relation between $10^3 \times \ln(\alpha_{H2O\text{-}H2})$ and AET_D in each fumarolic area is plotted in Fig. 3.

At Tarumae, where the highest outlet temperature of 609°C was recorded in this study, the calculated AET_D was 626°C. These values agree well with each other (Table 1). We

conclude that the re-equilibration via reaction (1.1), almost reached the isotope exchange equilibrium under the outlet temperature of 609°C at this fumarole.

On the other hand, the calculated AET_D (287°C) at E-san was rather different from the observed highest outlet temperature (107°C) in Field X of E-san. This overestimation when fumarole outlet temperatures are <400°C is not inconsistent with the results of other work (see Figure 4). The most probable reason for this overestimation is that the fumarolic gases had been at the AET_D temperature near the surface but were then quenched by some sudden cooling event (such as mixing with meteoric water *etc.*) just prior to venting from the fumarole (Mizutani, 1983). The highest outlet temperature of 225°C observed in Field Y of E-san (Mambo and Yoshida, 1993) also suggests that the fumarolic gases had been at a temperature of about the AET_D (287°C) near the surface. The reaction rate of equation (1.1) at the lower temperature (107°C) would be too slow to allow re-equilibration.

In case of Kuju, where an outlet temperature of 203°C was recorded in this study, the calculated AET_D (185°C) was similar to the observed outlet temperature (Table 1). We conclude that the reaction (1.1) almost reached the isotope exchange equilibrium at 203°C, even though this temperature is lower than 400°C. With the exception of results from the Showashinzan volcano, previous work shows that for fumarole outlet temperatures of 200 - 400°C there is usually reasonably close agreement of temperature and $\delta D(H_2)$ values close to the isotope exchange equilibrium with coexisting fumarolic H_2O at the temperatures of outlet (Fig. 4). While the reaction rate of equation (1.1) would be slow below 400°C, the key is probably whether there is sufficient time for re-equilibration before emission, and these results seem to indicate that for this fumarole, there was indeed sufficient time.

In conclusion, we can apply the AET_D as a tracer of temperature to fumaroles with outlet temperatures greater than 200°C. We are able to estimate accurate outlet temperatures for fumaroles having outlet temperatures of more than 400°C from their AET_D. On the other hand, for fumaroles having outlet temperatures of between 200 and 400°C, the quality of the

359 estimates are dependent on the residence time of the fumarolic fluids/gases within volcano,
360 since the final reduction of temperature at depths until emission from fumaroles. For the
361 fumaroles for which the outlet temperatures is as low as 200°C, for instance, the potential
362 errors of up to 150°C on the calculated AET_D are possible (Fig. 4). For fumaroles having
363 outlet temperatures of less than 200°C, significant deviations from the outlet can be expected.
364 Even for the fumaroles for which the outlet temperatures are less than 200°C, the
365 absolute δD values of fumarolic H_2 and their temporal variation can provide important
366 information about the magmatic/hydrothermal system under the volcano. For instance, we can
367 estimate the temperature of fumarolic gases at depths just prior to cooling, from the $\delta D(H_2)$
368 value (e.g. Mizutani, 1983; Taran et al., 2010). Furthermore, we can detect variations in the
369 temperature of fumarolic gases prior to the cooling by continuous monitoring the δD values of
370 fumarolic H_2.
371 The difference of AET_D from the actual temperatures of the outlets (200–400°C) of
372 fumaroles of Showashinzan volcano reported in the literature may have a different
373 explanation. It is possible that contamination of the δD value by $\delta D(CH_4)$ could be an
374 alternative possible cause. Under this scenario, while H_2 attained isotope exchange
375 equilibrium with fumarolic H_2O at temperatures as low as 200°C, the contribution of
376 fumarolic CH_4 to H_2 during δD analysis could have increased the observed $\delta D(H_2)$ values of
377 the 200–400°C fumaroles and thus AET_D (see Appendix for the detail). If so, we could extend
378 our application of AET_D as a tracer of temperature to the fumaroles to reliably predict
379 temperatures at outlet temperatures as low as 200°C, *e.g.* the Kuju volcano, see above. To
380 verify this possibility, further studies on fumarolic H_2 are needed, especially for those in
381 fumaroles showing the outlet temperatures between 200 and 400°C.
382
383 **4.2 H_2 in the Volcanic Plumes**

Both concentrations and δD values of H_2 in the plume samples were presented in Table 2, together with the approximate distance to the fumarole from which each plume cloud apparently derived. All the plume samples can be characterized by significant enrichment in H_2. The average H_2 concentration of the plume samples taken apparently within the volcanic plume in each volcano were for Tarumae, 17 ppm (from 0.65 ppm to 47.6 ppm, n = 7), for Kuju 4.6 ppm (from 0.62 ppm to 13.0 ppm, n = 5), for E-san 16 ppm (from 0.49 ppm to 82.9 ppm, n = 7), and 1.2 ppm (from 0.54 ppm to 2.3 ppm, n = 12) for Aso. Those samples taken apparently outside the volcanic plume were 0.51 ppm, 0.53 ppm, 0.53 ppm, and 0.53 ppm respectively. The highest H_2 concentration in each area was always obtained at the sampling points closest to the targeted fumarole, usually at distances less than 1 m. While most of the samples showed significant H_2 enrichment, the air samples taken outside the volcanic plume exhibited H_2 concentrations close to the minimum in each area, indeed close to those in background tropospheric air (*ca*. 0.5 ppm; Novelli *et al*., 1999). We concluded that fumarolic H_2 was the source of the excess H_2 in the plume samples. That is to say, variations in the mixing ratios of fumarolic gases within ambient air resulted in the variable H_2 concentrations in the plume samples. The average (maximum) mixing ratios of fumarolic H_2 within the total H_2 of the plume were roughly estimated to be 97 (99)% at Tarumae, 89 (96)% at Kuju, 97 (99)% at E-san, and 59 (78)% at Aso, assuming that the excess H_2 corresponds to fumarolic H_2 in each plume sample.

This conclusion was also supported by the δD values of the H_2 in the plume samples. As shown in Figure 5, the reciprocal of the H_2 concentration in the plume samples showed a good linear relationship with the δD values. Similar linear relationships between the reciprocal of concentrations and their isotopic compositions were recognized in H_2 from urban atmospheres (Gerst and Quay, 2001). The linear relationships suggested that both the concentrations and the δD values of H_2 in the samples from each site can be explained by simple mixing between two end-members, both of which can be classified to a single category at least for the δD

values of H_2 (e.g. Keeling, 1958; Tsunogai et al., 1998; Tsunogai et al., 2003; Tsunogai et al., 2005; Tsunogai et al., 2010). Furthermore, the H_2-depleted end-member seems to be almost common irrespective of the volcano under study, showing an H_2 concentration of ca. 0.5 ppm and D-enriched δD values of around +100 ‰. The H_2-depleted end-member must be H_2 in background tropospheric air, certainly both compare well with literature values (Gerst and Quay, 2001; Rice *et al.*, 2010). On the other hand, the H_2-enriched end-member containing highly D-depleted H_2 (compared to background tropospheric H_2) must be the fumarolic H_2, because fumarolic H_2 are always characterized by lower δD values than those in the tropospheric H_2 (Table 1).

By extrapolating the linear relationship between $1/H_2$ and δD to $1/H_2 = 0$ to exclude the contribution of the tropospheric H_2 (the H_2-depleted end-member) from the δD value of each sample (e.g. Keeling, 1958; Tsunogai et al., 2003), we estimated the δD values of fumarolic H_2 (the H_2-enriched end-member) to be –260 ± 30‰ at Tarumae, –509 ± 23‰ at Kuju, and –437 ± 14‰ at E-san (Fig. 5) through the least squares fitting of strait lines. Because the data errors were variable especially in $1/[H_2]$, we fitted each line taking into account the differences in the errors (York, 1966).

The $1/H_2$ values of the fumarolic H_2 were larger than 0, which means that the δD values of the H_2-enriched end-members must be larger than the δD values estimated. The $1/H_2$ values of the fumarolic H_2 were around 10^{-4} (ppm^{-1}) and the slopes of the linear fitted relationships (Fig. 5) were always less than +500‰ per ppm^{-1} so that the differences were less than 0.05‰. As a result, we disregarded this difference and used 0 for the $1/H_2$ value of the H_2-enriched end-members.

The estimated δD values of Tarumae, Kuju, and E-san corresponded to those in each fumarolic H_2 within the error of the fitting (Fig. 5). We concluded that each fumarolic H_2 was the only source of the excess H_2 in each volcanic plume. Furthermore, δD values of fumarolic H_2 were always quenched in volcanic plume without interactions with the other components,

436 including H_2O in volcanic plume, during mixing with ambient air, hence holding the same δD
437 values as those at the fumarole. As a result, we can deduce the δD value of fumarolic H_2
438 without sampling of fumarolic gases directly, by determining both the concentrations and the
439 δD values of H_2 in its volcanic plume and correcting the contribution of the tropospheric H_2
440 from the δD values as we did in Tarumae, Kuju, and E-san.
441 It is possible that each volcanic plume cloud derived from not one (targeted) fumarole,
442 but from many fumaroles located in each fumarolic area. That is to say, the excess H_2 in the
443 plume samples could comprise most of the fumarolic H_2 from nearby fumaroles. This could
444 lead to heterogeneities in the outlet temperatures in a fumarolic area, which could change the
445 δD values of fumarolic H_2 estimated from the plume.
446 However, as shown above, each end-member δD value estimated from the plume H_2
447 corresponded to those of the targeted fumarole (Fig. 5). Furthermore, all the plume samples
448 showed good linear correlation on the mixing line (Fig. 5). As a result, contribution of
449 fumarolic H_2 from the nearby low temperature fumaroles seems to be minimal. This is
450 especially true at Kuju and E-san, probably because of the depletion of H_2 in the low
451 temperature fumaroles (*e.g*. Giggenbach, 1987; Symonds *et al*., 1994; Taran *et al*., 1995). It is
452 also possible that the emission fluxes might be smaller from the low temperature fumaroles
453 than the targeted ones. In conclusion, we have shown that the end-member δD value deduced
454 from the plume H_2 is close to the δD value of H_2 in the fumarole showing highest outlet
455 temperature in each fumarolic area.
456
457 **4.3 Application to Remote Temperature Sensing on the Aso Volcano**
458 By extrapolating the linear relationship between $1/H_2$ and δD in the plume samples
459 taken at Aso to $1/H_2 = 0$, we estimated the average δD value of fumarolic H_2 to be –172 ±
460 16‰ (Fig. 5). The δD value of fumarolic H_2 was much higher than that of the 609°C fumarole
461 at Tarumae (–247 ‰), but much lower than that of the tropospheric H_2. We concluded that the

462 major source of the excess H_2 in the volcanic plume were the fumaroles at the bottom of the
463 crater. By applying the average δD value of magmatic H_2O obtained from the active
464 volcanoes in convergent margins (–24.5 ± 7.3‰) (the average and the 1 σ dispersion range of
465 the fumarolic H_2O in high temperature fumaroles on convergent-plate volcanoes; Giggenbach,
466 1992), we estimated the AET_D of the Aso fumaroles to be 868 ± 97°C. While the range of δD
467 value applied to the fumarolic H_2O in Aso was assumed from the high-temperature fumaroles
468 in the volcanoes on convergent margins worldwide, the value is reasonable for H_2O in such
469 locally occurring high-temperature fumaroles as well. This includes those in high-temperature
470 fumaroles of nearby volcanoes within the possible variation range, such as those at the
471 Satsuma-Iwojima volcano showing an outlet temperature more than 800°C (from –31 to
472 –23‰; Shinohara *et al*., 2002), and at the Kuju volcano, showing the outlet temperatures of
473 more than 480°C (–18.9 ‰ and –17.0‰; Mizutani *et al*., 1986).

474 Neither direct sampling of fumarolic gases nor direct measurement of fumarolic
475 temperatures have been practical in the deep crater of Aso. Instead, remote sensing has been
476 employed at the crater edge in past studies, at distances of about 200 m from the fumarolic
477 area (Mori and Notsu, 1997; Saito *et al*., 2005; Furukawa, 2010; Shinohara *et al*., 2010). The
478 highest temperature of the fumarolic area at Aso (Fig. 2), has been monitored periodically (at
479 least monthly) by the Japan Metrological Agency (JMA) since 1993 using a dedicated IR
480 thermometer (operating at wavelengths of 8–13 μm). That work reported that the outlet
481 temperature was ca. 300°C in Nov., 2010 when we took our plume samples (Japan
482 Meteorological Agency, 2010). Although the highest temperature of the fumarolic area at the
483 Aso volcano as determined by JMA has varied widely in past, showing the maximum of ca.
484 500°C in 2003 and 2009, and a minimum of less than 100°C in 1999 and 2006. It is true
485 though, that the highest temperature determined by JMA was much lower than the AET_D we
486 estimated from the fumarolic area.

487 On the other hand, some glowing spots (red glow) have been observed with the unaided
488 human eye at night in the fumarolic area at times since November 2000. Given this, the
489 temperature of the red glow must be more than 500°C (Saito *et al*., 2005). The latest
490 observation of red glow prior to our sampling was in May, 2010. Therefore, that the
491 temperatures determined by JMA (*e.g*. *ca*. 350°C in May, 2010) must be lower than the actual
492 outlet, by at least 150°C. Furthermore, Mori and Notsu (2008) determined CO/CO_2 ratios of
493 the fumarolic gases at the Aso volcano remotely using FT-IR on six occasions from 1996 to
494 2003, and estimated the equilibrium temperature of fumarolic gases was almost stable at
495 670°C to 870°C, using the empirical relation between the equilibrium temperatures and
496 CO/CO_2 ratios in the fumarolic gases. Shinohara *et al*. (2010) also obtained similar
497 equilibrium temperatures from 750°C to 950°C for the fumarolic gases during the
498 observations from 2006 and 2009 using both H_2/H_2O ratios and SO_2/H_2S ratios in the
499 volcanic plume determined by using a portable multi-sensor system (Shinohara, 2005).
500 Although the equilibrium temperatures could be higher than the outlet to some extent (*e.g*.
501 Symonds *et al*., 1994), both the presence of the red glow only 5 months before and the
502 equilibrium temperatures close to the AET_D suggest that the calculated AET_D was a
503 reasonable estimate of the fumarole outlet temperatures.

504 The azimuthal resolution of the IR thermometer of JMA is 1°, and this corresponds to a
505 spatial resolution of more than 1 m at their measurements at the distance of *ca*. 200 m from
506 the fumarolic area. The dimension of each fumarole at the surface must be much less than 1 m
507 (Furukawa, 2010), so that the lower spatial resolution as compared to the dimension of each
508 fumarole is likely to be responsible for the lower temperatures in the IR thermometer
509 measurements of JMA. This hypothesis is also supported by the observation on the fumarolic
510 area using a high resolution IR thermometer having *ca*. two order of magnitude better
511 resolution than that of JMA instrument (Saito *et al*., 2005). The highest temperature of up to
512 800°C was detected on November 2003 (Saito *et al*., 2005), when the highest temperature

513 determined by JMA was only 350°C. Although the estimated temperatures using the high
514 resolution IR thermometer decreased to less than 500°C in September 2003, and less than
515 300°C in March 2005 (Furukawa, 2010), we concluded that the AET_D (868 ± 97°C in Nov.
516 2010) represented the highest outlet temperature of the fumaroles at Aso and that further
517 reduction in the dimensions of the fumaroles at the surface has been responsible for the
518 declines in the temperatures determined by using the high-resolution IR thermometer since
519 September 2003. That is to say, temporal variation in the dimensions of fumaroles at surface,
520 probably because of variation in the emission flux of fumarolic gases, was responsible for the
521 temporal variation in the temperature determined by the IR thermometers, as well as the
522 appearance/disappearance of the red glow. Hence we conclude that the actual outlet
523 temperature of the Aso fumaroles keeps the temperature close to the chemical equilibrium
524 temperature between H_2-H_2O, SO_2-H_2S, and CO-CO_2. These features of the fumarolic area at
525 the Aso volcano resemble those at the Satsuma-Iwojima volcano, which is characterized by
526 the continuous, long-term emission of volcanic gases from the fumaroles. The highest outlet
527 temperatures vary very little being around 850°C (*e.g.* Shinohara *et al*., 1993), and also have
528 the accompanying "red glows" on the fumarolic area.
529
530 **4.4 Application to Remote Temperature Sensing on Volcanic Fumaroles in general**
531 Our observations on the Aso plume suggest that the average δD value of fumarolic H_2
532 for a fumarolic area should be amenable to estimation with a similar precision as that at Aso
533 (less than ±20‰) from those in the plume, provided the plume is enriched in H_2 to a similar
534 degree as is the Aso plume (from 0.54 ppm to 2.3 ppm). This means that the excess H_2 (*i.e.*
535 the fumarolic H_2) occupies 59 % (on average) and 78 % (maximum) of total H_2 in the plume.
536 The observed H_2 enrichment in the Aso plume was not a special characteristic limited to Aso,
537 but is fairly general. For example, the average excess H_2 in comparison with the ambient
538 atmospheric H_2 in the July 29, 1980 plume (non-eruptive) of Mount St. Helens, for instance,

539 was +0.59 ppm at 16 km downwind from the fumarolic area (McGee, 1992), so that the
540 average mixing ratio of fumarolic H_2 within total H_2 in the plume was greater than 50 %
541 (calculated assuming the H_2 concentration of ambient air to be 0.5 ppm H_2; Novelli *et al.,*
542 1999). Because the average mixing ratio is very similar to that in the Aso plume samples we
543 obtained in this study, we could estimate the δD values of fumarolic H_2 of Mount St. Helens
544 precisely, with a similar precision to that at Aso (± 16‰), if we had sampled the plume of
545 Mount St. Helens at the distances of 16 km downwind from the fumarolic area and
546 determined both concentrations and δD values of H_2 in the plume in 1980.

547 Sufficient H_2 enrichment in volcanic plumes derived from high-temperature volcanic
548 fumaroles is a promising way ahead. The H_2/H_2O ratio in the fumarolic gases at Aso,
549 estimated from those in the plume to be 10^3 to 10^4 μmol/mol (Shinohara *et al*., 2010), can be
550 classified as having a lower H_2/H_2O ratio than most of the high-temperature fumarolic gases
551 in world volcanoes, such as St. Augustine (5,800 μmol/mol), Etna (11,000 μmol/mol), Merapi
552 (12,000 μmol/mol), Momotombo (4,700 μmol/mol), St. Helens (5,300 μmol/mol), Poas
553 (5,800 μmol/mol), Showashinzan (1,900 μmol/mol), Usu (3,200 μmol/mol), Ardoukoba
554 (22,000 μmol/mol), Erta' Ale (22,000 μmol/mol), Nyiragongo (34,000 μmol/mol), Surtsey
555 (27,000 μmol/mol), Kilauea summit lava lake (15,000 μmol/mol), and Kilauea East Rift Zone
556 (12,000 μmol/mol), [mean values of those compiled in Symonds *et al*. (1994)]. Thus, as far as
557 the extent of dilution by ambient air is the similar, we can anticipate similar H_2 enrichment
558 (more than a 50% contribution of fumarolic H_2 in the plume H_2 on average) in a typical
559 volcanic plume.

560 In the case of low temperature fumaroles, the concentrations of fumarolic H_2 are small
561 in general (*e.g*. Giggenbach, 1987; Symonds *et al.*, 1994; Taran *et al*., 1995). As a result, the
562 estimation on fumarolic $\delta D(H_2)$ from H_2 in the volcanic plume might be difficult for them
563 because of the small H_2 enrichment in the plume. However, even if the plume is too depleted
564 in H_2 at the point where it is safe enough to sample by hand, recent advances in remote

565 sampling tools such as manned aerial vehicles (*e.g.* Fiske and Sigurdsson, 1982; Shinohara *et*
566 *al.*, 2003; Wardell *et al.*, 2004), unmanned aerial vehicles (e.g. Saiki and Ohba, 2010),
567 balloons (*e.g.* Belousov and Belousova, 2004), and robots (*e.g.* Muscato *et al.*, 2003) could be
568 utilized to take more concentrated samples in places where people cannot safely go.

569 In the case of high temperature fumaroles, care must be taken when the variation in δD
570 values under the isotope exchange equilibrium becomes relatively insensitive to temperature
571 variation, especially for those having temperatures exceed 1,000 °C (Fig. 3). That is to say,
572 variations in $\delta D(H_2)$ values in response to the same degree of temperature variation becomes
573 relatively smaller at higher temperatures. In the case of Aso, for instance, we estimated the
574 outlet temperature (868 °C) within an error of 97°C, by using both the fumarolic $\delta D(H_2)$ with
575 an error of 16‰ and the fumarolic $\delta D(H_2O)$ with an error of 7.3‰ (see section 4.3 for the
576 detail). Even if we determined both $\delta D(H_2)$ and $\delta D(H_2O)$ in a fumarole with the same degree
577 of errors as those in the case of Aso (±16‰ and ±7.3‰, respectively), the error accompanied
578 in its estimated temperature would be ca. ±120 °C when the outlet temperature was 1,000 °C,
579 and ca. ±170 °C when the outlet temperature was 1,200 °C. As a result, for the fumaroles
580 having elevated outlet temperatures, we have to estimate fumarolic $\delta D(H_2)$ more precisely
581 from H_2 in the volcanic plume, to attain a similar precision to that of with Aso (smaller than
582 ±100 °C). For instance, precisions smaller than 11‰ and 6‰ are needed for 1,000 °C and
583 1,200 °C fumaroles, respectively, to attain a similar precisions to those of Aso. The
584 concentrations of fumarolic H_2 are large in general in the high temperature fumaroles (*e.g.*
585 Giggenbach, 1987; Symonds *et al.*, 1994; Taran *et al.*, 1995). As a result, precise estimation
586 of fumarolic $\delta D(H_2)$ from H_2 in the volcanic plume might be possible.

587 In addition to the problem of insensitivity to temperature variation in the high
588 temperature region, care must be taken because no reliable fractionation factors are available
589 at temperatures greater than 1,300 °C (Richet et al., 1977). To apply HIReTS to fumaroles
590 having temperatures greater than 1,300 °C, we must calculate/estimate equilibrium

591 fractionation factors for the temperatures greater than 1,300 °C. However, 1,300 °C is
592 sufficient as the upper limit to determine the temperature for most of the volcanic fumaroles
593 throughout the world.

594 The δD value of fumarolic H_2 estimated from plume samples will enable us to estimate
595 the highest outlet temperature of the fumaroles of interest if the temperature exceed 400 °C,
596 assuming the isotope exchange equilibrium between the fumarolic H_2 and fumarolic H_2O. For
597 the estimation of temperature, however, data on the δD value of fumarolic H_2O is also
598 essential. In contrast to H_2, it is rather difficult to estimate δD value of fumarolic H_2O from
599 the plume because the concentration of H_2O in background air is much higher than that of H_2,
600 about 10^3 to 10^4 ppm is usual. Furthermore, both concentrations and δD values of H_2O in air
601 can be quite varied. Based on the knowledge obtained on the fumarolic H_2O from past studies,
602 however, we can estimate the value precisely in several ways outlined below.

603 In case of fumarolic H_2O in high-temperature magmatic discharges on convergent-plate
604 volcanoes, we can assume an approximate δD value from the literature to be –24.5±7.3‰ (the
605 average and the 1 σ variation range of the fumarolic H_2O in high-temperature fumaroles on
606 convergent-plate volcanoes; Giggenbach, 1992). This is the same data previously applied to
607 Aso in section 4.3. It may be that such a general δD value for H_2O cannot be applied to the
608 fumarolic H_2O studied. However, because H_2O is the major component in most fumarolic
609 fluids and the alternative end-member is local meteoric water, we can restrict the most
610 extreme δD value from the magmatic fluids to that of local meteoric water (Giggenbach,
611 1992; Goff and McMurtry, 2000). Furthermore, because H_2O is the major component in
612 fumarolic gases that have fumarolic H_2/H_2O ratios less than 0.04 (*e.g.* Symonds *et al.*, 1994),
613 typical variation range of δD values in fumarolic H_2O are much narrower than that of
614 fumarolic H_2 (e.g. Bottinga, 1969; Mizutani, 1983; Giggenbach, 1992; Taran et al., 1995;
615 Kiyosu and Okamoto, 1998; Goff and McMurtry, 2000; Taran et al., 2010). As a result, we
616 can approximate the δD values of fumarolic H_2O to be uniform irrespective of variations in

617 the temperature of fumaroles. In the case of the decline in temperature over time shown at
618 Showashinzan and Nasudake, which was discussed in section 1, for example, while $\delta D(H_2)$
619 declined at the rates of –1.9±1.0‰/yr at Showashinzan and –12.9±2.5‰/yr at Nasudake,
620 $\delta D(H_2O)$ showed little variation, with values of –0.4±0.8 ‰/yr and –1.8±1.0 ‰/yr,
621 respectively (Mizutani, 1983). Hence, it may be that if some past data on the $\delta D(H_2O)$ were
622 available for a particular fumarolic area, the values could be applicable to the present as well.
623 It may also be that we could use the δD value of magmatic H_2O estimated for the volcano
624 using alternative methods: such as measuring that found in fresh volcanic rocks (*e.g.* Newman
625 *et al.*, 1983; Taylor *et al.*, 1983; Kusakabe *et al.*, 1999). Furthermore, H_2 data alone is
626 sufficient to estimate relative temperature variation. In conclusion, we can remotely estimate
627 the temperature of the fumaroles (or at least for their temporal variations) at a distance based
628 only on H_2 in the plume.
629
630 **4.5 Comparison with the Traditional Methods**
631 Our method using Hydrogen Isotopes for Remote Temperature Sensing (HIReTS) has
632 significant advantages over traditional remote sensing methods, *e.g.* using IR radiation. The
633 described method in particular overcomes the problems of remote and accurate temperature
634 measurement of fumaroles that have small dimensions, or to which there is no direct
635 line-of-sight, as shown in section 4.3 for Aso. In contrast to some of the IR thermometers,
636 which cannot determine temperature during daytime (Saito *et al.*, 2005), it is possible to
637 determine the temperature at any time, day or night, using HIReTS. Furthermore, field work
638 at volcanoes becomes simpler: one just needs to bring more than a few evacuated 300 mL
639 glass bottles (200 g for each) to a point downstream of the fumarolic area and open the seal.
640 Most of the advantages of HIReTS described above are applicable to the other remote
641 temperature sensing methods that determine the chemical compositions of fumarolic gases
642 remotely and estimate the equilibrium temperature (*e.g.* Mori and Notsu, 1997; Shinohara,

643 2005). In practice, however, it is difficult to deduce accurate and precise fumarolic
644 concentrations for all of the components of the chemical equilibrium from those in the plume.
645 This is especially true when the measurements on the plume are being done at a distance from
646 the fumarolic area (Symonds *et al*., 1994). As a result, the estimate of equilibrium
647 temperature comes with significant errors (*e.g*. ±150 to ±200°C; Mori and Notsu (2008)).
648 Furthermore, the equilibrium temperature is the temperature at depth - potentially somewhat
649 higher than that at the outlet (*e.g*. Symonds *et al*., 1994). While the information on the
650 equilibrium temperature is useful in many respects, HIReTS is preferable to determine the
651 outlet temperature of fumaroles remotely.

652 On the other hand, the disadvantage of using HIReTS compared to the traditional
653 methods is the time needed to determine temperature. While most of the IR thermometers can
654 determine the temperature on site, the HIReTS methodology needs more than a few days to
655 estimate temperature for a fumarolic area subsequent to the field and laboratory work. Also,
656 to avoid potentially large errors (see section 4.1), prior to applying HIReTS, we would have
657 to verify the fumarolic temperature to be more than 400°C (or at least more than 200°C),
658 using some alternative method, such as a traditional IR thermometer. Furthermore, ambiguity
659 in the δD values of fumarolic H_2O could reduce the accuracy of the absolute temperature
660 obtained from HIReTS in some volcanoes.

661 In conclusion, HIReTS can be a better or only choice for remote temperature sensing of
662 fumaroles in many volcanoes, but care must be exercised because each applications is likely
663 to be different. It would be better to combine HIReTS with the other traditional methods
664 during the actual temperature sensing in field. Moreover, to be certain of collecting plume
665 samples enriched in H_2, it might be preferable to measure H_2 concentration real-time during
666 the field work at volcanoes, applying some portable sensors (Shinohara et al., 2010).
667
668 **5. CONCLUSIONS**

669 For a fumarolic area in a volcano having outlet temperatures of more than 400°C, we
670 can remotely estimate an accurate temperature of the fumaroles by using HIReTS developed
671 in this study. This method estimates the δD value of fumarolic H_2 from those in the plume. It
672 is possible that HIReTS can be expanded to temperatures as low as 200°C in the future,
673 although it will depend on the results of further studies on fumarolic H_2. HIReTS can be a
674 better or indeed the only choice for accurate remote temperature sensing of fumaroles at many
675 volcanoes. Furthermore, even for fumaroles showing temperatures lower than the HIReTS
676 lower limit, we can obtain novel information concerning the magmatic/hydrothermal systems
677 under the volcano. However, as we have to presume the δD value of fumarolic H_2O without
678 actual measurement to obtain absolute temperature of these fumaroles using HIReTS, the
679 accuracy of temperatures estimated by HIReTS could be worse for fumaroles for which we
680 cannot presume accurate δD values for fumarolic H_2O.
681
682 **Acknowledgments**
683 The fundamental idea of this study was first tested by Mr. H. Tatewaki (Hokkaido Univ.) in
684 his graduation thesis. Discussions with Drs. H. Shinohara (AIST), T. Mori (Univ. Tokyo), M.
685 Kusakabe (Toyama Univ.), and Y. Taran (UNAM) were very helpful. We would like to thank
686 Drs. Y. Fushiya (Sapporo District Meteorological Observatory), K. Imamura (Aso City
687 Center), S. Abe (Aso Crater Observatory), J. Nishijima (Kyushu Univ.), S. Ehara (Kyushu
688 Univ.), S. Ohsawa (Kyoto Univ.), J. Yamamoto (Kyoto Univ.), U. Konno (AIST), S. Daita
689 (Hokkaido Univ.), H. Sakuma (Hokkaido Univ.), A. Suzuki (Hokkaido Univ.), T. Izuta
690 (Hokkaido Univ.), and R. Ueda (Hokkaido Univ.) for their valuable support for sampling in
691 the volcanoes and Drs. T. Ohba (Tokai Univ.), R. Botcharnikov (Univ. Hannover), and an
692 anonymous reviewer for critical reading of and valuable remarks on an earlier version of this
693 manuscript. This study was supported by MEXT Scientific Research Program Nos. 23740399
694 and 23241001, and JSPS Japan-Russia Research Cooperation Program.

APPENDIX

The data set on AET_D in high-temperature volcanic fumaroles used in this study (Fig. 4) was compiled from past work and did not include the AET_D data from the Kuju volcano reported by Mizutani (1983), in which the AET_D estimated at the Kuju volcano were very different from that at the outlet. The observed outlet temperature was 151°C, but AET_D was 790°C, in 1964. While Mizutani (1983) proposed that the AET_D represented the elevated temperature in the gas reservoir at depth below the Kuju volcano, we concluded that the values were affected by artifacts and hence removed them from the figures and discussions of this paper. Our reasons for this were:

(1) The δD values of fumarolic H_2 reported for the same Field A in Mizutani (1983) showed significant deviation from those that we determined in this study (2010).

(2) Because of the little apparent variation in Field A of the Kuju volcano since 1964, (highest outlet temperatures were 183°C in 1964, 214°C in 1984, 200°C in 2000, and 203°C in this study; Mizutani *et al*., 1986; Amita and Ohsawa, 2003), it is difficult to attribute such significant variation in the δD values of fumarolic H_2 between Mizutani (1983) and this study to temporal variation in the fumarolic H_2.

The most important difference between Mizutani (1983) and this study is the analytical method employed to determine the $\delta D(H_2)$ values. While our method did not include gases other than H_2 in the determined $\delta D(H_2)$ values, the $\delta D(H_2)$ values used by Mizutani (1983) was the total δD value of the gases that had not dissolved in NaOH solution during sampling. These gases included H_2, N_2, CO, Ar, He, and CH_4. As a result, the differences of the $\delta D(H_2)$ value produced by the method would be significant if the fumarolic gases contained elevated CH_4 relative to H_2. While Mizutani (1983) disregarded this possibility based on analytical results from only one fumarolic gas sample taken at a fumarole in Field C of the Kuju volcano in 1961 that showed an outlet temperature of 400°C and a CH_4/H_2 ratio of 0.0014. We

concluded that the actual CH_4/H_2 ratios of the samples, for which Mizutani (1983) determined $\delta D(H_2)$ values, were much higher than 0.0014 and that the $\delta D(H_2)$ value was contaminated by CH_4, and this was responsible for the elevated $\delta D(H_2)$ values reported in that work. Our reasons for thinking this are:

(1) While the sample showing the CH_4/H_2 ratio of 0.0014 was taken at 1961, the samples for which Mizutani (1983) determined $\delta D(H_2)$ values were taken during 1964 to 1967. Because the CH_4/H_2 ratios at the fumaroles on the Kuju volcano increased to 0.04–2.0 in their subsequent observation on August 1984 (Mizutani *et al.*, 1986), the CH_4/H_2 ratios during 1964 to 1967 would have been much larger than 0.0014.

(2) While the sample showing the low CH_4/H_2 ratio of 0.0014 was taken at a fumarole with an outlet temperature of 400°C, the samples for which Mizutani (1983) determined the δD values of H_2 were taken at fumaroles with outlet temperatures from 121 to 360°C. Because the CH_4/H_2 ratios at Kuju tended to increase in proportionally with the decrease in the outlet temperatures (the CH_4/H_2 ratio of a fumarole showing an outlet temperature of 170°C in 1984, for example, was 2.0; Mizutani *et al*., 1986), the samples for which he determined $\delta D(H_2)$ values could have more elevated CH_4/H_2 ratios.

(3) Because the $\delta D(CH_4)$ value is much higher than $\delta D(H_2)$ value under the hydrogen isotope exchange equilibrium (Richet *et al.*, 1977), contamination of fumarolic H_2 by fumarolic CH_4 might enhance observed $\delta D(H_2)$ values and thus AET_D.

To test our hypothesis, we recalculated the $\delta D(H_2)$ value and AET_D for the 151°C fumarole; using 2 for the actual CH_4/H_2 ratio (that of a 170°C fumarole at Kuju determined in 1984) and –100 ‰ for the $\delta D(CH_4)$ value (the δD value of CH_4 in deep-sea hydrothermal fluids; Welhan and Craig, 1983). The $\delta D(CH_4)$ value also corresponds to the $\delta D(CH_4)$ value that is at isotope exchange equilibrium with coexisting fumarolic H_2O at 600°C. While Mizutani (1983) determined the $\delta D(H_2)$ value of this fumarole to be –185‰ and the AET_D

745 790°C, the recalculated $\delta D(H_2)$ value became –525‰, and the recalculated AET_D became
746 175°C; almost corresponding to the outlet (151°C). Thus, we concluded that all the $\delta D(H_2)$
747 values of Kuju in Mizutani (1983) were affected by artifacts, such as contamination of CH_4 to
748 the $\delta D(H_2)$ values.

749 The problems on the CH_4 contamination could also have impacted some past $\delta D(H_2)$
750 data of low temperature fumaroles (< 400°C), such as those in the Showashinzan volcano.
751 The AET_D in the 200–400°C fumaroles correspond to the outlet in most of the volcanoes,
752 except the Showashinzan volcano (see Fig. 4). While the $\delta D(H_2)$ data included fumaroles
753 showing outlet temperatures less than 400°C (Mizutani, 1983), data on the CH_4/H_2 ratio were
754 from those of more than 500°C in the volcano (Mizutani and Sugiura, 1982). Because
755 $\delta D(CH_4)$ is much higher than the $\delta D(H_2)$ under the isotope exchange equilibrium as stated
756 above, CH_4 contamination is likely to be responsible for the overestimated AET_D as well.
757 Differ from the Kuju volcano, however, it is difficult to verify $\delta D(H_2)$ again in the
758 Showashinzan volcano at present. As a result, further studies on the other volcanoes are
759 needed to compare the AET_D with the outlet temperatures of the fumaroles showing
760 200–400°C, as presented in section 4.2.
761

Table 1
Chemical and isotopic compositions of fumarolic gas samples, together with apparent equilibrium temperature calculated for $\delta D(H_2O)$ and $\delta D(H_2)$ (AET_D).

		temp. (°C)	H_2/H_2O (μmol/mol)	$\delta D(H_2O)$ (‰)	$\delta D(H_2)$ (‰)	AET_D (°C)
Tarumae	Vent A	609	811	–33.4	–247.0 ±0.6	626
Kuju	Field A	203	47	–44.3 ±1.0	–527.7 ±10.1	185
E-san	X field	107	18	–35.3	–432.1 ±2.5	287

Table 2
Chemical and isotopic compositions of H_2 in volcanic plume samples.

No.	distance* (m)	H_2 (ppm)	$\delta D(H_2)$ (‰)	Remark
		Tarumae volcano		
TA-01	50	0.51	+86.2	Background air
TA-02	50	2.1	-187.3	
H-16	15	12.5	-244.7	
K-13	8	34.3	-243.3	
H-91	3	19.0	-246.4	
H-89	3	2.1	-219.1	
K-07	1	47.6	-226.3	
H-87	100	0.65	-40.8	
		Kuju volcano		
ASO-04	>10	0.53	+61.9	Background air
K-10	5	0.62	-47.1	
H-28	1	4.4	-438.0	
K-91	1	13.0	-477.4	
K-07	3	2.9	-410.5	
K-13	3	2.0	-364.5	
		E-san volcano		
H-16	1	7.8	-394.4	
H-28	1	17.7	-424.0	
K-13	3	0.68	-66.1	
H-87	10	0.53	+69.5	
K-07	20	0.53	+70.1	Background air
H-89	50	0.89	-134.8	
H-91	>100	0.49	+96.2	
H-53	0.3	82.9	-435.1	
		Aso volcano		
ASO-C07	150	0.61	+44.1	A#
ASO-C08	150	2.1	-104.5	A#
ASO-C05	150	1.0	-27.2	A#
ASO-C09	150	1.1	-31.9	A#
ASO-C02	150	1.2	-46.9	A#
ASO-C10	300	0.54	+98.7	E#
ASO-C04	150	0.54	+94.8	F#, Background air
ASO-C01	150	0.52	+107.7	F#, Background air
ASO-01	300	2.3	-99.5	D#
ASO-02	200	2.1	-99.6	C#
ASO-03	200	0.67	+44.2	C#
H-04	300	1.6	-83.1	D#
TGA08	200	0.77	-6.5	B#
H-87	150	0.94	-45.7	A#

* approximate distance from the targeted fumarole.
# the sampling point shown in Fig. 2.

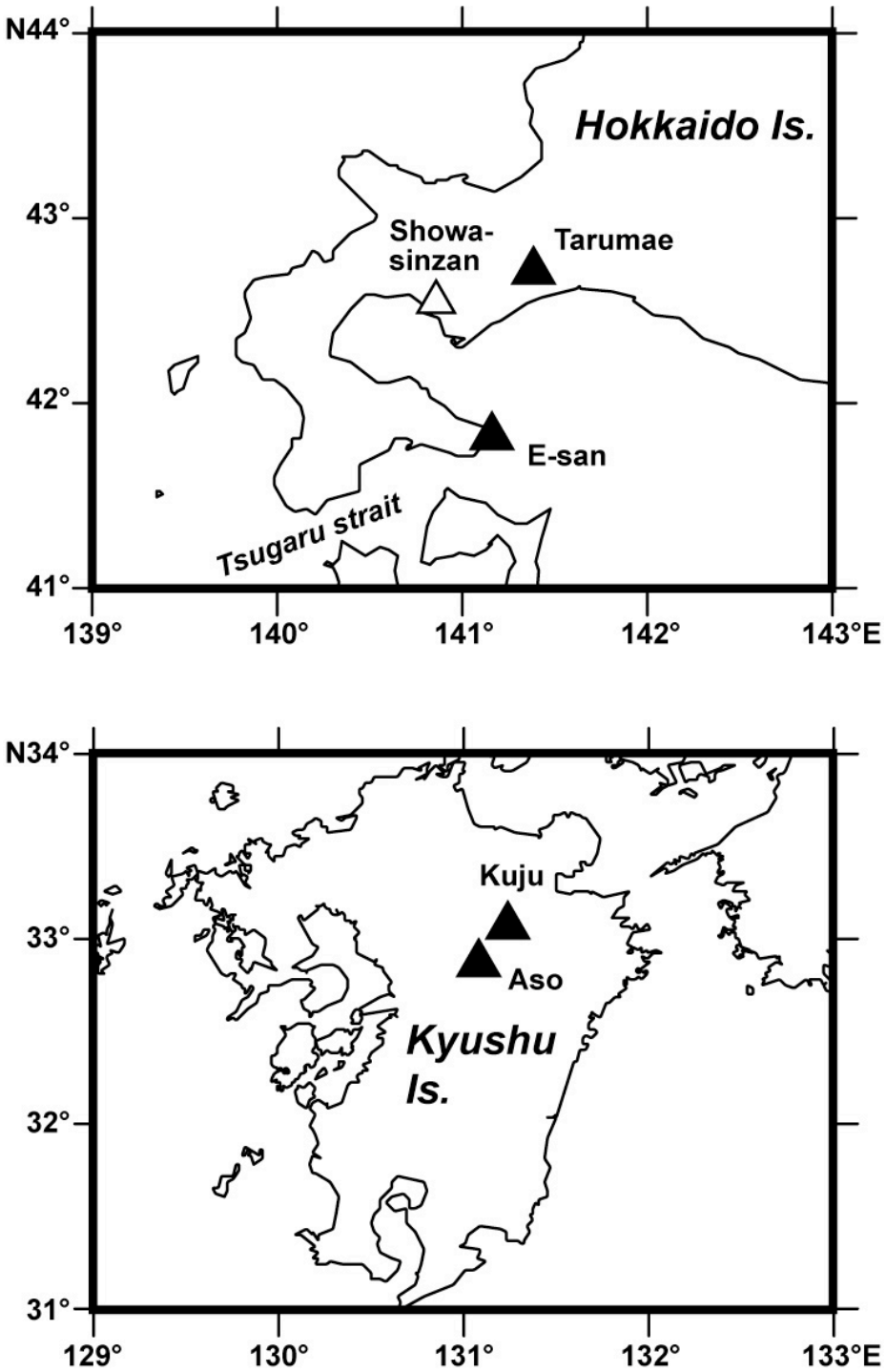

Fig. 1

A map showing the location of the study volcanoes.

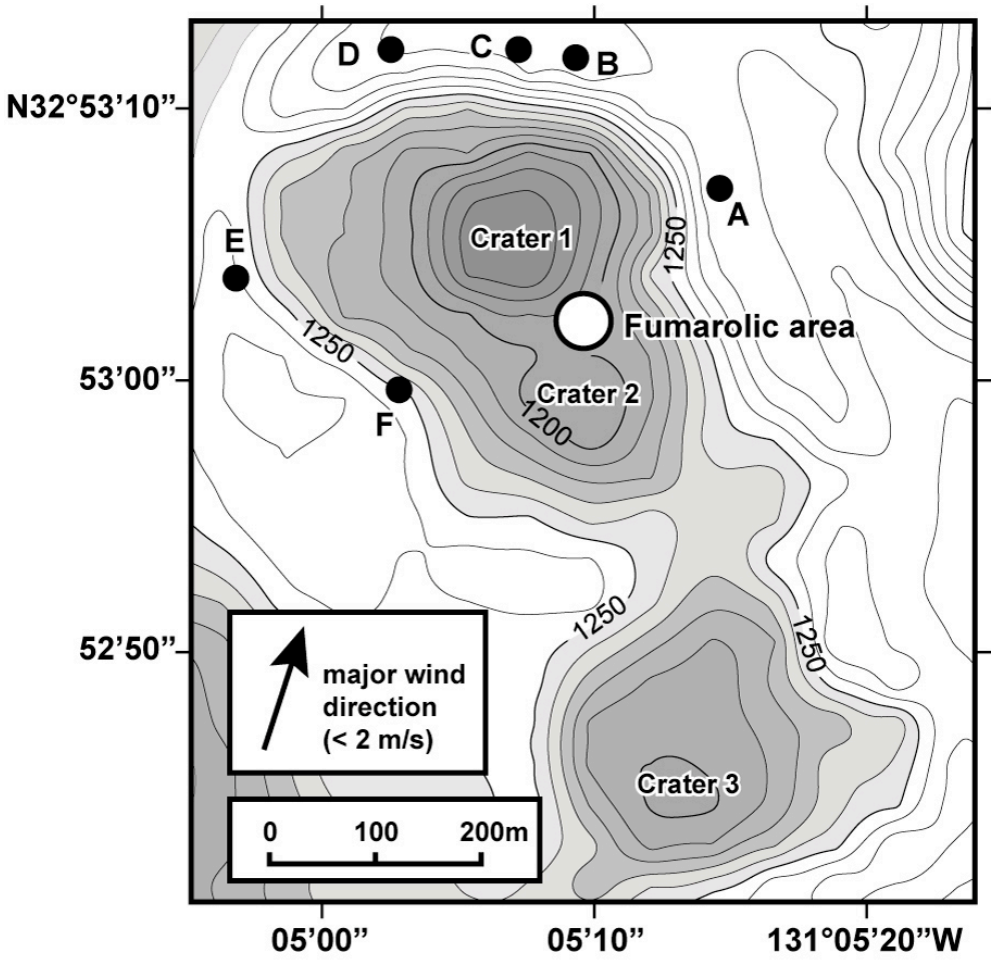

Fig. 2

A topographic map showing the summit area of Mt. Naka-dake, Aso volcano, together with the sampling points of the volcanic plume samples shown by the solid circles (points A to F) and the major wind direction during sampling. The open circle on the south-eastern part of the Crater 1 shows the location of the major fumarolic area.

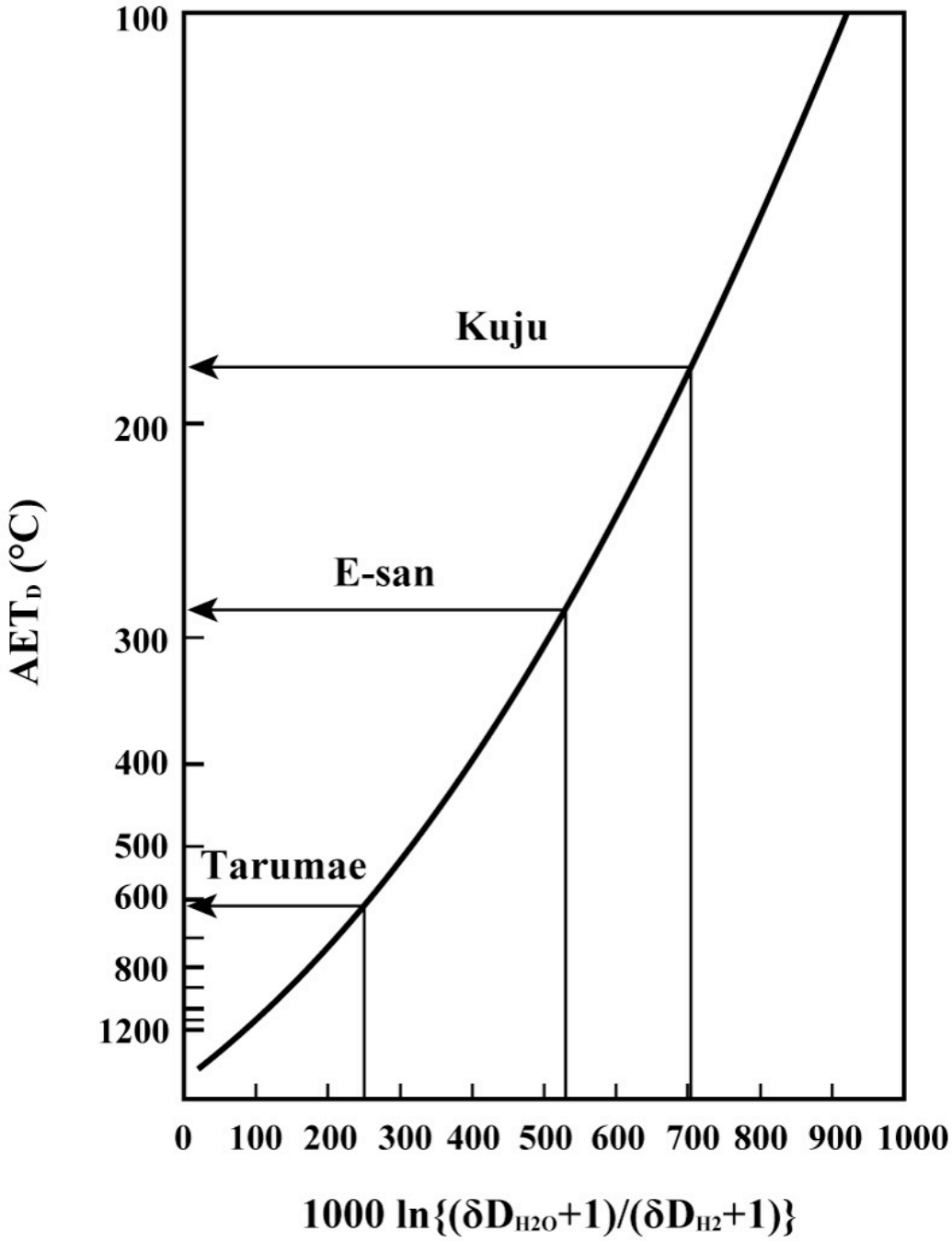

Fig. 3

Relationships between the apparent equilibrium temperature assuming hydrogen isotope exchange equilibrium between H_2O and H_2 (AET_D) and the value of $1000\ln\{(\delta D_{H2}+1)/(\delta D_{H2O}+1)\}$, estimated from the fractionation factors in Richet *et al.* (1977) .

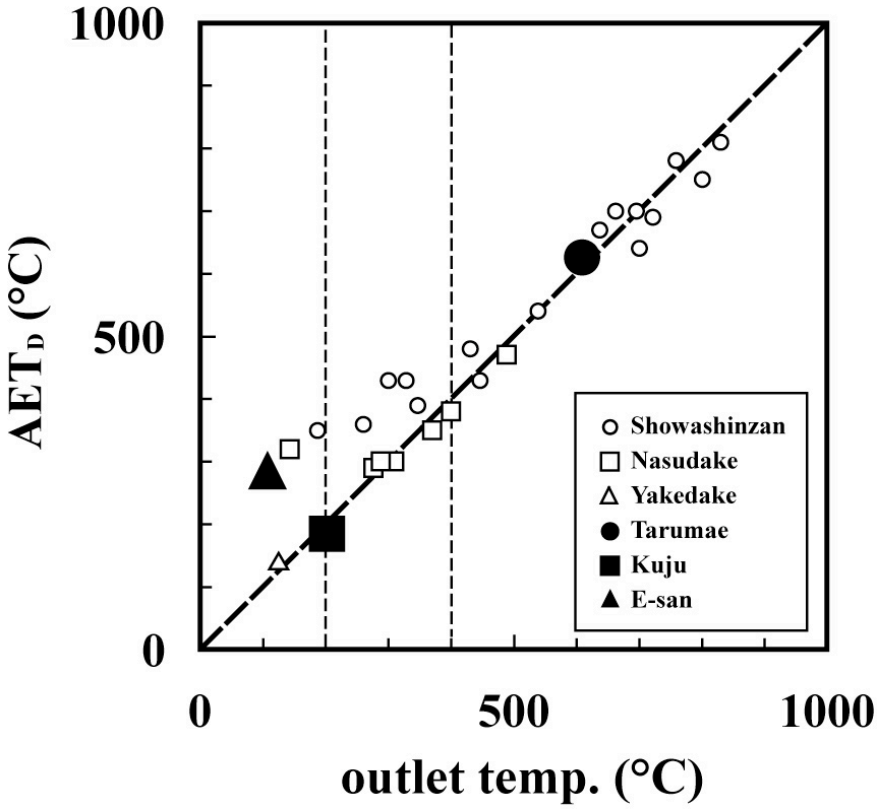

Fig. 4

The calculated temperatures assuming isotope exchange equilibrium between H_2 and H_2O in fumarolic gases (AET_D) determined in this study (black circle: Tarumae, black square: Kuju, black triangle: E-san) plotted as a function of the outlet temperatures of fumaroles, together with those determined in Mizutani (1983) (open circles: Showashinzan, open squares: Nasudake, open triangles: Yakedake), except for Kuju in the literature (see Appendix for the rationale).

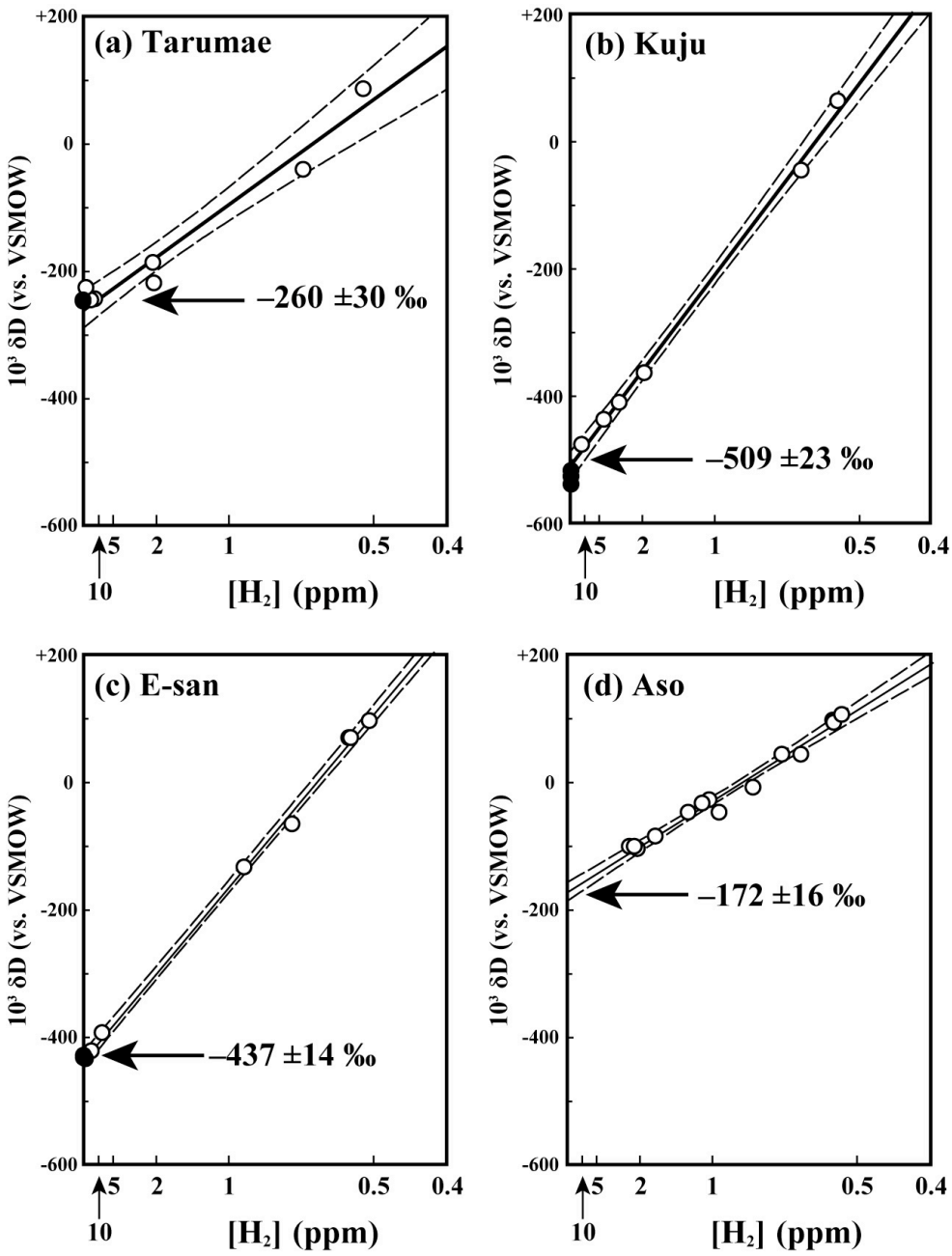

Fig. 5

Relationship between δD of H_2 and the reciprocal of H_2 concentration in the volcanic plume of Tarumae (a), Kuju (b), E-san (c), and Aso (d) (open circles), together with those in each fumarole (solid circles). Each solid line is the least squares fitting of the plume samples, while each dotted line is the 2 σ variation envelop of the fitting line.

References:

Amita K. and Ohsawa S. (2003) Mixing Process of Air and Underground Water into Magmatic Gas Discharged from Kuju-Iwoyama Fumarolic Area of Kuju Volcano, Central Kyushu, Japan. *J. Geotherm. Res. Soc. Japan* **25**, 245-265 (in Japanese with English abstract).

Belousov A. and Belousova M. (2004) The first attempt of sampling of volcanic cloud. *Priroda* **4**, 42-54 (in Russian).

Botcharnikov R. E., Shmulovich K. I., Tkachenko S. I., Korzhinsky M. A. and Rybin A. V. (2003) Hydrogen isotope geochemistry and heat balance of a fumarolic system: Kudriavy volcano, Kuriles. *J. Volcanol. Geotherm. Res.* **124**, 45-66.

Bottinga Y. (1969) Calculated fractionation factors for carbon and hydrogen isotope exchange in the system calcite - carbon dioxide - graphite - methane - hydrogen - water vapor. *Geochim. Cosmochim. Acta* **33**, 49-64.

Connor C. B., Clement B. M., Xiaodan S., Lane S. B. and West T. J. (1993) Continuous monitoring of high-temperature fumaroles on an active lava dome, Volcan Colima, Mexico: evidence of mass flow variation in response to atmospheric forcing. *J. Geophys. Res.* **98**, 19713–19722.

Coplen T. B. (2008) *IUPAC Provisional Recommendations: Explanatory glossary of terms used in expression of relative isotope ratios and gas ratios*. Commission on Isotopic Abundances and Atomic Weights, IUPAC, (also available at http://old.iupac.org/reports/provisional/abstract08/coplen_310508.html).

Coplen T. B. and Hopple J. (1995) Audit of VSMOW distributed by the United States National Institute of Standards and Technology. In *Reference and intercomparison materials for stable isotopes of light elements (Proceedings of a consultants meeting held in Vienna, 1-3 December 1993)*. IAEA, Viena. pp. 51-66.

Ellis A. J. (1957) Chemical equilibrium in magmatic gases. *Am. J. Sci.* **255**, 416-431.

Fischer W. A., Moxham R. M., Polcyn F. and Landis G. H. (1964) Infrared surveys of Hawaiian volcanoes. *Science* **146**, 733-742.

Fiske R. S. and Sigurdsson H. (1982) Soufriere Volcano, St. Vincent: Observations of Its 1979 Eruption from the Ground, Aircraft, and Satellites. *Science* **216**, 1105-1106.

Furukawa Y. (2010) Infrared thermography of the fumarole area in the active crater of the Aso volcano, Japan, using a consumer digital camera. *J. Asian Earth Sci.* **38**, 283-288.

Gelwicks J. T. and Hayes J. M. (1990) Carbon-isotopic analysis of dissolved acetate. *Anal.*

Chem. **62**, 535-539.

Gerst S. and Quay P. (2001) Deuterium component of the global molecular hydrogen cycle. *J. Geophys. Res.* **106**, 5021–5031.

Giberti G., Jaupart C. and Sartoris G. (1992) Steady-state operation of Stromboli volcano, Italy. *Bull. Volcanol.* **54**, 535–541.

Giggenbach W. F. (1987) Redox processes governing the chemistry of fumarolic gas discharges from White Island, New Zealand. *Appl. Geochem.* **2**, 143–161.

Giggenbach W. F. (1992) Isotopic shifts in waters from geothermal and volcanic systems along convergent plate boundaries and their origin. *Earth Planet. Sci. Lett.* **113**, 495-510.

Giggenbach W. F. and Goguel R. L. (1989) *Collection and analysis of geothermal and volcanic water and gas discharges. Report No. CD 2401*. Chemistry Division, Department of Scientific and Industrial Research, Petone, New Zealand.

Goff F. and McMurtry G. M. (2000) Tritium and stable isotopes of magmatic waters. *J. Volcanol. Geotherm. Res.* **97**, 347-396.

Harris A. J. L., Lodato L., Dehn J. and Spampinato L. (2009) Thermal characterization of the Vulcano fumarole field. *Bull. Volcanol.* **71**, 441-458.

Hedenquist J. W. and Aoki M. (1991) Meteoric interaction with magmatic discharges in Japan and the significance for mineralization. *Geology* **19**, 1041-1044.

Hirota A., Tsunogai U., Komatsu D. D. and Nakagawa F. (2010) Simultaneous determination of $\delta^{15}N$ and $\delta^{18}O$ of N_2O and $\delta^{13}C$ of CH_4 in nanomolar quantities from a single water sample. *Rapid Commun. Mass Spectrom.* **24**, 1085-1092.

Ishimura T., Tsunogai U. and Gamo T. (2004) Stable carbon and oxygen isotopic determination of sub-microgram quantities of $CaCO_3$ to analyze each individual foraminiferal shell. *Rapid Commun. Mass Spectrom.* **18**, 2883-2888.

Itai T. and Kusakabe M. (2004) Some practical aspects of an on-line chromium reduction method for D/H analysis of natural waters using a conventional IRMS. *Geochem. J.* **38**, 435-440.

Japan Meteorological Agency (2010) *Monthly Report on Earthquakes and Volcanoes in Japan: November, 2010*. Japan Meteorological Agency, Tokyo (in Japanese, also available at www.seisvol.kishou.go.jp/tokyo/volcano.html).

Kawagucci S., Toki T., Ishibashi J., Takai K., Ito M., Oomori T. and Gamo T. (2010) Isotopic variation of molecular hydrogen in 20-375 °C hydrothermal fluids as detected by a new analytical method *J. Geophys. Res.* **115**, doi: 10.1029/2009JG001203.

Kawagucci S., Tsunogai U., Kudo S., Nakagawa F., Honda H., Aoki S., Nakazawa T. and Gamo T. (2005) An analytical system for determining delta^{17}O in CO_2 using continuous flow-isotope ratio MS. *Anal. Chem.* **77**, 4509 -4514.

Keeling C. D. (1958) The concentration and isotopic abundances of atmospheric carbon dioxide in rural areas. *Geochim. Cosmochim. Acta* **13**, 322-334.

Kiyosu Y. (1983) Hydrogen isotopic compositions of hydrogen and methane from some volcanic areas in northeastern Japan. *Earth Planet. Sci. Lett.* **62**, 41–52.

Kiyosu Y. and Okamoto Y. (1998) Variation in fumarolic H_2 gas and volcanic activity at Nasudake in Japan. *J. Volcanol. Geotherm. Res.* **80**, 27-37.

Komatsu D. D., Tsunogai U., Yamaguchi J. and Nakagawa F. (2005) Stable carbon isotopic analysis of atmospheric methyl chloride using CF-IRMS by using selective removal of unsaturated hydrocarbons. *Rapid Commun. Mass Spectrom.* **19**, 477-483.

Komatsu D. D., Ishimura T., Nakagawa F. and Tsunogai U. (2008) Determination of the $^{15}N/^{14}N$, $^{17}O/^{16}O$, and $^{18}O/^{16}O$ ratios of nitrous oxide by using continuous-flow isotope-ratio mass spectrometry. *Rapid Commun. Mass Spectrom.* **22**, 1587-1596.

Kusakabe M., Sato H., Nakada S. and Kitamura T. (1999) Water contents and hydrogen isotopic ratios of rocks and minerals from the 1991 eruption of Unzen volcano, Japan. *J. Volcanol. Geotherm. Res.* **89**, 231-242.

Mambo V. S. and Yoshida M. (1993) Behavior of arsenic in volcanic gases. *Geochem. J.* **27**, 351-359.

Matsubaya O., Sakai H., Ueda A., Tsutsumi M., Kusakabe M. and Sasaki A. (1978) Stable isotope study of the hotsprings and volcanoes of Hokkaido, Japan. *Papers Inst. Thermal Spring Res., Okayama Univ.* **47**, 55-67 (in Japanese with English abstract).

Matsuo S. (1961) On the chemical nature of fumarolic gases of Volcano Showashinzan, Hokkaido, Japan. *J. Earth Sci., Nagoya Univ.* **9**, 80-100.

McGee K. A. (1992) The structure, dynamics, and chemical composition of noneruptive plumes from Mount St. Helens, 1980–1988. *J. Volcanol. Geotherm. Res.* **51**, 269-282.

Menyailov I. A., Nikitina L. P., Shapar V. N. and Pilipenko V. P. (1986) Temperature increase and chemical change of fumaloric gases at Momotombo volcano, Nicaragua, in 1982–1985: are these indicators of a possible eruption? *J. Geophys. Res.* **91**, 12199-12214.

Mizutani Y. (1983) Deuterium fractionation between water vapor and hydrogen gas in fumarolic gases. *Geochem. J.* **17**, 161-164.

Mizutani Y. and Sugiura T. (1982) Variations in chemical and isotopic composition of

fumarolic gases from Showashinzan volcano, Hokkaido, Japan. *Geochem. J.* **16**, 63-71.

Mizutani Y., Hayashi S. and Sugiura T. (1986) Chemical and isotopic compositions of fumarolic gases from Kuju-Iwoyama, Kyushu, Japan. *Geochem. J.* **20**, 273-285.

Mori T. and Notsu K. (1997) Remote CO, COS, CO_2, SO_2, HCl detection and temperature estimation of volcanic gas. *Geophys. Res. Lett.* **24**, 2047-2050.

Mori T. and Notsu K. (2008) Temporal variation in chemical composition of the volcanic plume from Aso volcano, Japan, measured by remote FT-IR spectroscopy. *Geochem. J.* **42**, 133-140.

Muscato G., Caltabiano D., Guccione S., Longo D., Coltelli M., Cristaldi A., Pecora E., Sacco V., Sim P., Virk G. S., Briole P., Semerano A. and White T. (2003) ROBOVOLC: A robot for volcano exploration result of first test campaign. *The Industrial Robot* **30**, 231-242.

Newman S., Epstein S. and Stolper E. (1983) Water, carbon dioxide, and hydrogen isotopes in glasses from the ca. 1340 A.D. eruption of the Mono Craters, California: Constraints on degassing phenomena and initial volatile content. *J. Volcanol. Geotherm. Res.* **35**, 75-96.

Novelli P. C., Lang P. M., Masarie K. A., Hurst D. F., Myers R. and Elkins J. W. (1999) Molecular hydrogen in the troposphere: Global distribution and budget. *J. Geophys. Res.* **104**, 30,427-30,444.

Ohba T., Hirabayashi J. and Yoshida M. (1994) Equilibrium temperature and redox state of volcanic gas at Unzen volcano, Japan. *J. Volcanol. Geotherm. Res.* **60**, 263-272.

Proskurowski G., Lilley M. D., Kelley D. S. and Olson E. J. (2006) Low temperature volatile production at the Lost City Hydrothermal Field, evidence from a hydrogen stable isotope geothermometer. *Chem. Geol.* **229**, 331-343.

Rahn T., Kitchen N. and Eiler J. (2002) D/H ratios of atmospheric H_2 in urban air: Results using new methods for analysis of nano-molar H_2 samples. *Geochim. Cosmochim. Acta* **66**, 2475-2481.

Rhee T. S., Mak J., Röckmann T. and Brenninkmeijer C. A. M. (2004) Continuous-flow isotope analysis of the deuterium/hydrogen ratio in atmospheric hydrogen. *Rapid Commun. Mass Spectrom.* **18**, 299-306.

Rice A., Quay P., Stutsman J., Gammon R., Price H. and Jaeglé L. (2010) Meridional distribution of molecular hydrogen and its deuterium content in the atmosphere. *J. Geophys. Res.* **115**, doi:10.1029/2009JD012529.

Richet P., Bottinga Y. and Javoy M. (1977) A review of hydrogen, carbon, nitrogen, oxygen, sulphur, and chlorine stable isotope fractionation among gaseous molecules. *Ann. Rev. Earth Planet. Sci.* **5**, 65-110.

Ripepe M., Harris A. J. L. and Carniel R. (2002) Thermal, seismic and infrasonic evidences of variable degassing rates at Stromboli volcano. *J. Volcanol. Geotherm. Res.* **118**, 285–297.

Saiki K. and Ohba T. (2010) Development of an Unmanned Observation Aerial Vehicle (UAV) as a Tool for Volcano Survey. *Bull. Volcanol. Soc. Jpn.* **55**, 137-146.

Saito G., Shinohara H. and Kazahaya K. (2002) Successive sampling of fumarolic gases at Satsuma-Iwojima and Kuju volcanoes, southwest Japan: Evaluation of short-term variations and precision of the gas sampling and analytical techniques. *Geochem. J.* **36**, 1-20.

Saito T., Sakai S., Iizawa I., Suda E., Umetani K., Kaneko K., Furukawa Y. and Ohkura T. (2005) A new technique of radiation thermometry using a consumer digital camcorder: Observations of red glow at Aso volcano, Japan. *Earth Planets Space* **57**, e5-e8.

Shimozuru D. and Kagiyama T. (1976) Newly Deviced Infra-red Radiometer (ERI Type IR Ground-Scanner) and the Surface Temperature of the Mihara Crater, O-shima. *Bull. Volcanol. Soc. Japan, Second Series* **21**, 95-105 (in Japanese with English abstract).

Shinohara H. (2005) A new technique to estimate volcanic gas composition: plume measurements with a portable multi-sensor system. *J. Volcanol. Geotherm. Res.* **143**, 319-333.

Shinohara H., Kazahaya K. and Saito G. (2003) Variation of CO_2/SO_2 ratio in volcanic plumes of Miyakejima: Stable degassing deduced from heliborne measurements. *Geophys. Res. Lett.* **30**, doi:10.1029/2002GL016105.

Shinohara H., Yoshikawa S. and Miyabuchi Y. (2010) Degassing of Aso Volcano, Japan through an Acid Crater Lake: Differentiation of Volcanic Gas-Hydrothermal Fluids Deduced from Volcanic Plume Chemistry, Abstract V23A-2387. *Presented at 2010 Fall Meeting, AGU, San Francisco, Calif., 13-17 Dec.*

Shinohara H., Giggenbach W. F., Kazahaya K. and Hedenquist J. W. (1993) Geochemistry of volcanic gases and hot springs of Satsuma-Iwojima, Japan: Following Matsuo. *Geochem. J.* **27**, 271–285.

Shinohara H., Kazahaya K., Saito G., Matsushima N. and Kawanabe Y. (2002) Degassing activity from Iwodake rhyolitic cone, Satsuma-Iwojima volcano, Japan: Formation of

a new degassing vent, 1990-1999. *Earth Planets Space* **54**, 175-185.

Stevenson D. S. (1993) Physical models of fumarolic flow. *J. Volcanol. Geotherm. Res.* **57**, 139-156.

Symonds R. B., Rose W. I., Bluth G. J. S. and Gerlach T. M. (1994) Volcanic-gas studies: Methods, results, and applications. In *Volatiles in Magmas* (eds. M. R. Carroll and J. R. Holloway). Mineralogical Society of America. pp. 1–66.

Taran Y. A., Varley N. R., Inguaggiato S. and Cienfuegos E. (2010) Geochemistry of H_2- and CH_4-enriched hydrothermal fluids of Socorro Island, Revillagigedo Archipelago, Mexico. Evidence for serpentinization and abiogenic methane. *Geofluids* **10**, 542–555.

Taran Y. A., Hedenquist J. W., Korzhinsky M. A., Tkachenko S. I. and Shmulovich K. I. (1995) Geochemistry of magmatic gases from Kudryavy volcano, Iturup, Kuril Islands. *Geochim. Cosmochim. Acta* **59**, 1749-1761.

Taylor B. E., Eichelberger J. C. and Westrich H. R. (1983) Hydrogen isotopic evidence of rhyolitic magma degassing during shallow intrusion and eruption. *Nature* **306**, 541-545.

Tsunogai U., Ishibashi J., Wakita H. and Gamo T. (1998) Methane-rich plumes in Suruga Trough (Japan) and their carbon isotopic characterization. *Earth Planet. Sci. Lett.* **160**, 97-105.

Tsunogai U., Nakagawa F., Komatsu D. D. and Gamo T. (2002) Stable carbon and oxygen isotopic analysis of atmospheric carbon monoxide using continuous-flow isotope ratio MS by isotope monitoring of CO. *Anal. Chem.* **74**, 5695-5700.

Tsunogai U., Nakagawa F., Gamo T. and Ishibashi J. (2005) Stable isotopic compositions of methane and carbon monoxide in the Suiyo hydrothermal plume, Izu-Bonin arc: tracers for microbial consumption/production. *Earth Planet. Sci. Lett.* **237**, 326-340.

Tsunogai U., Hachisu Y., Komatsu D. D., Nakagawa F., Gamo T. and Akiyama K. (2003) An updated estimation of the stable carbon and oxygen isotopic compositions of automobile CO emissions. *Atmos. Environ.* **37**, 4901-4910.

Tsunogai U., Kosaka A., Nakayama N., Komatsu D. D., Konno U., Kameyama S., Nakagawa F., Sumino H., Nagao K., Fujikura K. and Machiyama H. (2010) Origin and fate of deep-sea seeping methane bubbles at Kuroshima knoll, Ryukyu forearc region, Japan. *Geochem. J.* **44**, 477-487.

Wardell L. J., Kyle P. R. and Chaffin C. (2004) Carbon dioxide and carbon monoxide emission rates from an alkaline intra-plate volcano: Mt. Erebus, Antarctica. *J. Volcanol. Geotherm. Res.* **131**, 109-121.

Welhan J. A. and Craig H. (1983) Methane, hydrogen, and helium in hydrothermal fluids at 21°N on the East Pacific Rise. In *Hydrothermal Processes at Seafloor Spreading Centers* (ed. P. A. Rona). Plenum Press, New York. pp. 391-406.

York D. (1966) Least-squares fitting of a straight line. *Can. J. Phys.* **44**, 1079-1086.